European Journal of Neuroscience, Vol. 19, pp. 2169–2178, 2004

Immunocytochemical localization of the α_{1A} subunit of the P/Q-type calcium channel in the rat cerebellum

Ákos Kulik,[1,2,4] Kazuhiko Nakadate,[2,*] Akari Hagiwara,[2,3] Yugo Fukazawa,[2] Rafael Luján,[5] Hiromitsu Saito,[6] Noboru Suzuki,[6,8] Akira Futatsugi,[7,8] Katsuhiko Mikoshiba,[7,8,9] Michael Frotscher[1] and Ryuichi Shigemoto[2,3,4]
[1]Department of Anatomy and Cell Biology, University of Freiburg, 79104 Freiburg, Germany
[2]Division of Cerebral Structure, National Institute for Physiological Sciences, and [3]Department of Physiological Sciences, the Graduate University for Advanced Studies (*Sokendai*), Myodaiji, Okazaki, Japan
[4]CREST, Japan Science and Technology Corporation, Kawaguchi, Japan
[5]Centro Regional de Investigaciones Biomédicas, Facultad de Medicina, Universidad da Castilla-La Mancha, Campus Biosanitario, Albacete, Spain
[6]Functional Genomics Institutes, Center for Life Science Research, Mie University, Tsu, Mie, Japan
[7]Ca^{2+} Oscillation Project, JST, Shirokanedai, Minato-ku, Tokyo, Japan
[8]RIKEN BSI, 2-1 Hirosawa, Wako, Saitama, and [9]Institute of Medical Science, University of Tokyo, Tokyo, Japan

Keywords: electron microscopy, parallel fibre, pre-embedding immunogold, Purkinje cell, quantitative analysis

Abstract

Among various types of low- and high-threshold calcium channels, the high voltage-activated P/Q-type channel is the most abundant in the cerebellum. These P/Q-type channels are involved in the regulation of neurotransmitter release and in the integration of dendritic inputs. We used an antibody specific for the α_{1A} subunit of the P/Q-type channel in quantitative pre-embedding immunogold labelling combined with three-dimensional reconstruction to reveal the subcellular distribution of pre- and postsynaptic P/Q-type channels in the rat cerebellum. At the light microscopic level, immunoreactivity for the α_{1A} protein was prevalent in the molecular layer, whereas immunostaining was moderate in the somata of Purkinje cells and weak in the granule cell layer. At the electron microscopic level, the most intense immunoreactivity for the α_{1A} subunit was found in the presynaptic active zone of parallel fibre varicosities. The dendritic spines of Purkinje cells were also strongly labelled with the highest density of immunoparticles detected within 180 nm from the edge of the asymmetrical parallel fibre–Purkinje cell synapses. By contrast, the immunolabelling was sparse in climbing fibre varicosities and axon terminals of GABAergic cells, and weak and diffuse in dendritic shafts of Purkinje cells. The association of the α_{1A} subunit with the glutamatergic parallel fibre–Purkinje cell synapses suggests that presynaptic channels have a major role in the mediation of excitatory neurotransmission, whereas postsynaptic channels are likely to be involved in depolarization-induced generation of local calcium transients in Purkinje cells.

Introduction

Influx of calcium through voltage-activated calcium channels is an important prerequisite for the regulation of signalling processes in neurons such as neurotransmitter release, protein phosphorylation and gene expression (Miller, 1987). Pharmacologically and kinetically distinct calcium channels are involved both in electrical signalling and in coupling electrical signals to changes in cytoplasmic calcium concentration (Dunlap *et al*., 1995). Physiological and molecular studies have defined low-threshold T-type calcium channels and high voltage-activated (HVA) calcium channels – referred to as L-, N-, P/Q- and R-type – in neurons (Jones, 1998). The HVA calcium channels are multisubunit proteins composed of α_1, α_2/δ, β and γ subunits (Catterall, 1998). The primary subunits (α_1) of neuronal calcium channels, designated $\alpha_{1A}(Ca_v2.1)$, $\alpha_{1B}(Ca_v2.2)$, $\alpha_{1C}(Ca_v1.2)$, $\alpha_{1D}(Ca_v1.3)$ and $\alpha_{1E}(Ca_v2.3)$, contain the domains necessary for the calcium-selective pore and the voltage sensors (Catterall, 2000). The α_{1A} subunit constitutes the P/Q-type channel and mediates calcium influx across pre- and postsynaptic membranes, thereby triggering neurotransmitter release and other neuronal responses (Dunlap *et al*., 1995; Catterall, 1998).

There is evidence for the implication of multiple types of HVA calcium channels in the induction of long-term depression (LTD) and for their role in the mediation of excitatory and inhibitory synaptic transmission in the rodent cerebellum (Konnerth *et al*., 1992; Takahashi & Momiyama, 1993; Mintz *et al*., 1995; Eilers *et al*., 1996; Hartell, 1996; Doroshenko *et al*., 1997; Stephens *et al*., 2001). Among these ion channels, the physiological implication of the most abundant P/Q-type calcium channel (Starr *et al*., 1991; Usowicz *et al*., 1992; Westenbroek *et al*., 1995) is of particular interest in the pre- and postsynaptic elements of the cerebellar cortex. Presynaptically, P/Q-type currents account for a large fraction of the total calcium current in granule cells (Randall & Tsien, 1995) and climbing fibre (CF) varicosities (Regehr & Mintz, 1994), indicating a role in the presynaptic

Correspondence: Dr Á. Kulik, [1]Department of Anatomy and Cell Biology, as above.
E-mail: Akos.Kulik@anat.uni-freiburg.de

[*]*Present address*: Department of Histology and Neurobiology, Dokkyo University School of Medicine, 880 Kitakobayashi, Mibu, Tochigi 321-0293, Japan

Received 4 November 2003, revised 11 February 2004, accepted 16 February 2004

doi:10.1111/j.1460-9568.2004.03319.x

regulation of transmitter release at both parallel fibre (PF)– and CF–Purkinje cell (PC) synapses (Regehr & Mintz, 1994; Mintz *et al*., 1995; Matsushita *et al*., 2002). Postsynaptically, P/Q-type channels comprise about 90% of the calcium channels found in PCs (Mintz *et al*., 1992b; Jun *et al*., 1999). This channel type has a role in the generation of dendritic spikes (Tank *et al*., 1988) and in the amplification of excitatory postsynaptic potentials (EPSPs) in the distal dendrites of PCs as proposed in a computer model (De Schutter & Bower, 1994).

Most of the information on the distribution of the α_{1A} subunit of the P/Q-type channels in the rat and mouse brains derived from *in situ* hybridization, toxin binding and light microscopic immunocytochemical studies (Stea *et al*., 1994; Nakanishi *et al*., 1995; Tanaka *et al*., 1995; Westenbroek *et al*., 1995; Ludwig *et al*., 1997; Craig *et al*., 1998). In the present work, an affinity-purified subunit-specific antibody was used to investigate the spatial distribution of the α_{1A} subunit on the plasma membrane of cerebellar neurons using pre-embedding electron microscopy in combination with the quantification of immunogold density on reconstructed profiles.

Materials and methods

Antibodies

A polyclonal antibody specific for the α_{1A} subunit of P/Q-type calcium channel was produced by Alomone Laboratories (Jerusalem, Israel). Briefly, the antibody was raised in rabbits against a synthetic peptide corresponding to an intracellular loop between domains II and III (amino acid residues 865–881/CNA1/) of the α_{1A} subunit (Mori *et al*., 1991; Starr *et al*., 1991) and then affinity purified on immobilized CNA1. To identify GABAergic neurons we used a monoclonal antibody to glutamic acid decarboxylase (GAD65, Chemicon, Temecula, CA, USA).

Immunoblot analysis

Immunoblot analysis was performed as described previously (Kulik *et al*., 2002). The crude membrane preparations from postnatal day 12 (P12) wild-type, α_{1A}-deficient mice brain, and adult rat cerebellum were separated by 5% SDS-PAGE and transferred to polyvinylidene difluoride (PVDF, Bio-Rad, Hercules, CA, USA) membranes. Preparation of the α_{1A}-deficient mice will be described elsewhere (A. Futatsugi *et al*., personal communication). The membranes were blocked with Block-Ace (Dainippon Pharmaceutical, Japan) and then reacted with the affinity-purified α_{1A} antibody (0.2 μg/mL). An alkaline phosphatase-labelled secondary antibody (1 : 5000, Chemicon) was used to visualize the reacted bands.

Animals

A total of 12 adult male Wistar rats (Charles River, Freiburg, Germany), two P14 wild-type and two P14 α_{1A}-deficient mice were used in the present study. Care and handling of the animals prior to and during the experimental procedures followed European Union regulations and was approved by the Animal Care and Use Committees of the authors' institutions.

Immunocytochemistry for light microscopy

Wild-type and α_{1A}-deficient mice were deeply anaesthetized with 35 mg/kg body weight of sodium pentobarbital and brains were immediately removed and frozen in dry ice. Parasagittal sections were cut with a cryostat microtome at 10 μm thickness, fixed for 30 min in 50 mM phosphate-buffered saline (PBS, pH 7.4) containing 4% paraformaldehyde, treated with PBS containing 0.1% Triton X-100, blocked with PBS containing 2.5% bovine serum albumin (BSA, Nacalai Tesque, Japan) and 2.5% normal goat serum (NGS, Vector Laboratories, Burlingame, CA, USA), and then incubated overnight at 4 °C with the anti-α_{1A} antibody (1.5 μg/mL). After several washes with PBS, sections were incubated with a horseradish-peroxidase (HRP)-conjugated antirabbit secondary antibody (1 : 200, Zymed, CA, USA) and then with 3,3′-diaminobenzidine tetrahydrochloride (DAB, 0.05%) (Dojindo, Kumamoto, Japan) and 0.03% hydrogen peroxide for 15 min. Three rats (250–280 g) were anaesthetized deeply with Narkodorm-n (180 mg/kg, i.p.) (Alvetra GmbH, Germany) and perfused transcardially first with 0.9% saline followed by a fixative containing 4% paraformaldehyde, 15% saturated picric acid, and 0.05% glutaraldehyde (Polysciences, Warrington, PA, USA) in 0.1 M phosphate buffer (PB, pH 7.3). Tissue blocks containing the cerebellum were cryoprotected in 30% sucrose in 0.1 M PB overnight at 4 °C. Blocks were freeze-thawed in liquid nitrogen and then sections were cut on a vibratome at a thickness of 40 μm. The sections were blocked with PBS containing 10% NGS and 0.1% Triton X-100. They were then incubated with 0.8 μg/mL antibody for α_{1A} in 25 mM PBS containing 3% NGS and 0.1% Triton X-100 overnight at room temperature. After washes in PBS, the sections were incubated with biotinylated goat antirabbit IgG antibody (1 : 100, Vector Laboratories) at room temperature for 2 h. The sections were then washed and reacted with avidin–biotin–peroxidase complex (ABC kit, 1 : 100, Vector Laboratories) at room temperature for 2 h. Subsequently, the sections were incubated in 50 mM Tris-buffer (TB, pH 7.3) containing 0.025% DAB (Sigma, St. Louis, MO, USA) and 0.003% hydrogen peroxide. Finally, the sections were air-dried and coverslipped.

Immunocytochemistry for electron microscopy

Adult male rats ($n = 9$), P14 wild-type and α_{1A}-deficient mice ($n = 2$) were perfused with the same solutions as described for light microscopy. After perfusion, the tissue blocks were washed in PB, then sections were cut on a vibratome at a thickness of 50 μm, and cryoprotected in a solution containing 25% sucrose and 10% glycerol in 50 mM PB. The sections were freeze-thawed and incubated in a blocking solution containing 20% NGS in 50 mM Tris-buffered saline (TBS, pH 7.3) for 1 h, followed by incubation with the primary antibody (2.0 μg/mL) diluted in TBS containing 3% NGS overnight at room temperature. After washing, the sections were incubated either with the biotinylated goat antirabbit IgG secondary antibody (1 : 50) for immunoperoxidase reaction, or with 1.4 nm gold-coupled goat antirabbit secondary antibody (1 : 100, Nanogold, Nanoprobes, Stony Brook, NY, USA) for immunogold reaction, and then reacted with the ABC (1 : 100) and HQ Silver kit (Nanoprobes), respectively. After treatment with OsO_4, the sections were stained with uranyl acetate, dehydrated and flat-embedded in epoxy resin (Durcupan ACM, Fluka, Sigma-Aldrich, Gillingham, UK). Ultrathin sections were cut (Reichert Ultracut S; Leica, Germany), and then analysed in a Philips CM100 electron microscope. For double immunoelectron microscopy, sections incubated in a mixture of anti-GAD65 (1 : 800) and anti-α_{1A} (2.0 μg/mL) antibodies were reacted first with the immunogold method for α_{1A} up to the silver enhancement and then incubated with the ABC followed by a peroxidase reaction for GAD65.

Controls

To document the specificity of the immunolabelling, two series of experiments were performed: (i) staining of sections obtained from the α_{1A}-deficient mice, and (ii) adsorption of the primary antibody with the antigen peptide. No immunolabelling was detected on sections derived from α_{1A}-deficient mice. After adsorption of the primary antibody with the antigen peptide (2 μg/mL), the specific immunostaining pattern was completely abolished.

Three-dimensional reconstruction

The three-dimensional (3D) reconstruction of rat PF varicosities, PFs, and PC dendrites and spines immunoreactive for α_{1A} was carried out from serial ultrathin sections covering a length of approximately 1.5–2.0 μm for each PF and varicosity and approximately 0.8–1.2 μm for dendrites and spines. In each case the first ultrathin section of the series was obtained from the surface of the 50-μm-thick section. For graphical presentations, reconstructions were carried out by using three-dimensional reconstruction imaging (TRI) software (Ratoc, Tokyo, Japan).

Quantification of α_{1A} immunoreactivity

Three samples were taken from the molecular layer of the rat cerebellum immunolabelled for α_{1A}. Serial ultrathin sections were cut from the surface (up to 2.5 μm depth) of the samples of PF varicosities ($n = 10$), PC dendritic shafts ($n = 3$) and spines ($n = 24$), which were reconstructed as described above. For each synapse made by the PF varicosity and PC spine, distances between immunoparticles and the closest edge of the synapse were measured along the surface of the 3D reconstructed images by using TRI software. Immunoparticles were allocated to 60-nm-wide bins along the surface of the reconstructed images starting at the edge of synaptic specializations. Density of immunoparticles was calculated by dividing the number of immunoparticles in each bin by the sampled surface area. Data taken from the three samples were pooled after confirming that the distribution of particles in each sample was not significantly different from those in the other samples ($P > 0.05$, Kolmogorov–Smirnov nonparametric test). Serial ultrathin sections of CF varicosities ($n = 15$) were prepared, then the area of synaptic specializations and the number of immunoparticles, localized to the presynaptic membrane specialization of the varicosities, were determined. The density of immunogold particles on the presynaptic active zone was calculated as described above.

Results

Immunoblot analysis

The specificity of the antibody, used in the present study, was verified with immunoblot analysis using membrane fractions from whole brains of P12 wild-type and α_{1A}-deficient mice, as well as adult rat cerebellum (Fig. 1A). In the wild-type mice brain and rat cerebellum, we found a major immunoreactive product of about 180 kDa, which disappeared after adsorption of the primary antibody with the antigen peptide (1 μg/mL, data not shown). Furthermore, the immunoreactive band was completely abolished in the α_{1A}-deficient mice, indicating specificity of the antibody to the α_{1A} subunit.

Light microscopic distribution of immunoreactivity for the α_{1A} subunit

The use of α_{1A} affinity-purified antibody revealed a specific pattern of immunostaining in the adult rat (Fig. 1B and C) and P14 wild-type mouse (Fig. 1D) cerebellum. The most intense immunoreactivity was observed in the molecular layer, where PC dendrites receive excitatory and inhibitory afferents. Cell bodies of PCs showed moderate labelling for α_{1A} (Fig. 1C and D), whereas the granule cell layer was weakly immunolabelled. No immunostaining for α_{1A} was observed in the white matter. In P14 α_{1A}-deficient mice, the specific immunolabelling pattern described above was completely abolished (Fig. 1E). In addition, after adsorption of the primary antibody with the antigen

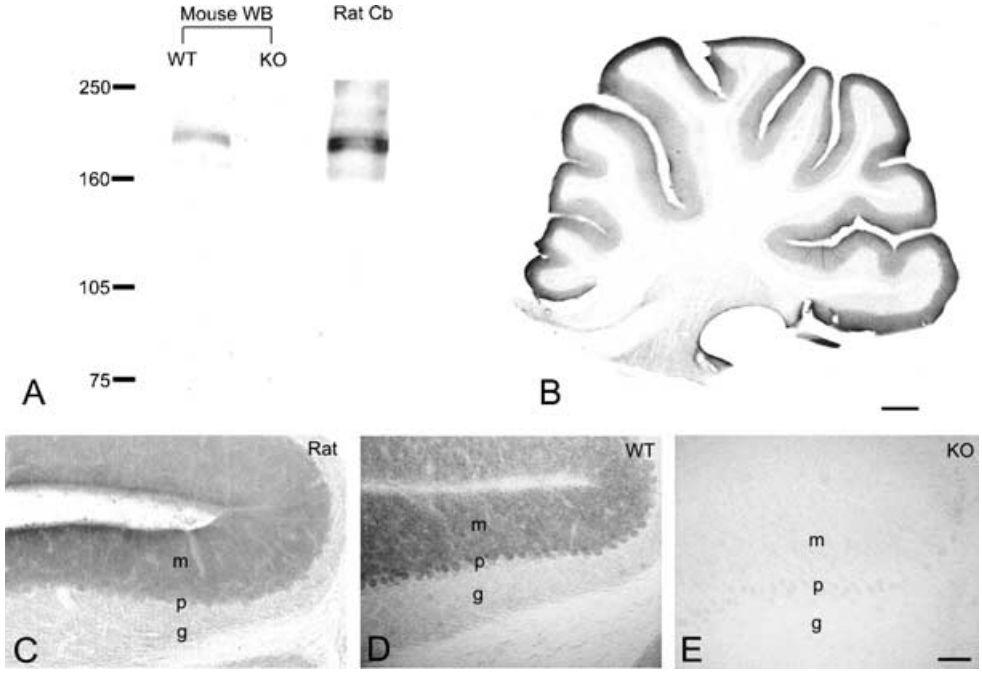

FIG. 1. Immunoblot analysis of whole brains of P12 wild-type, α_{1A}-deficient mice, and adult rat cerebellum, and the distribution of immunoreactivity for the α_{1A} subunit in the cerebellum. (A) Crude membrane preparations from whole brains (WB) of P12 wild-type (WT), α_{1A}-deficient mice (KO), and from adult rat cerebellum (Rat Cb) were subjected to 5% SDS-PAGE and transferred on to polyvinylidene difluoride filters. The filters were reacted with an anti-α_{1A} antibody. Immunoreactive products (about 180 kDa) were found in the brain of wild-type mice and rat cerebellum but not in the brain of α_{1A}-deficient mice. Positions of molecular mass markers (Amersham) in kDa are indicated on the left. (B–D) Strong immunoreactivity for α_{1A} is detected in the molecular layer (m), whereas the immunolabelling was moderate in the Purkinje cell layer (p) and weak in the granule cell layer (g). (E) No immunoreactivity for α_{1A} was found in the cerebellum of the α_{1A}-deficient mice. Scale bars, 500 μm (B) and 100 μm (C–E).

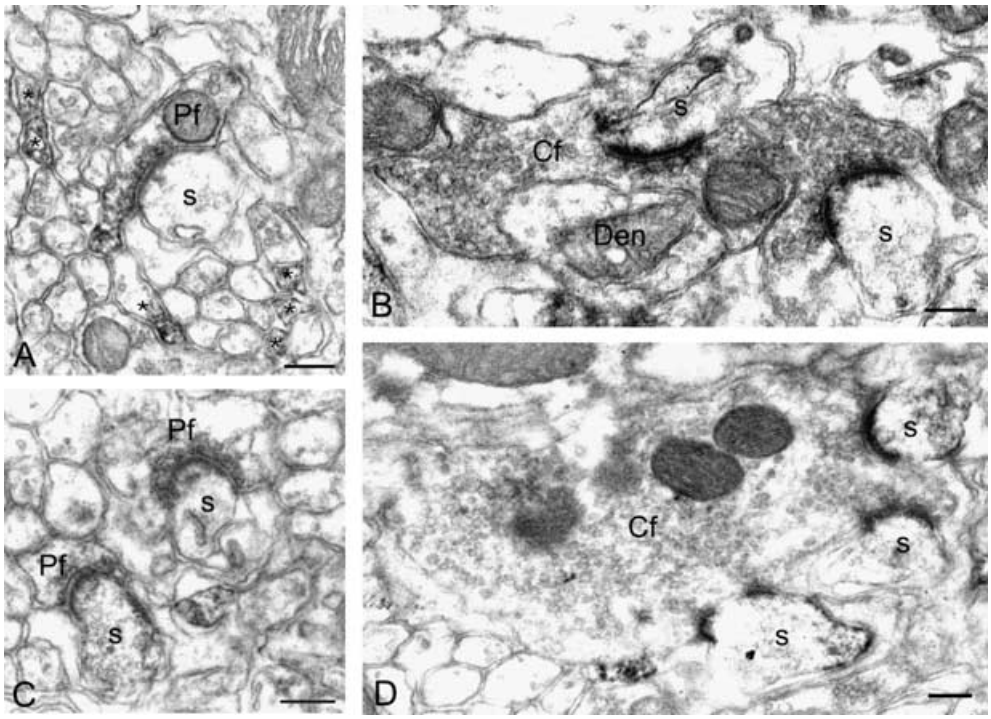

FIG. 2. Electron micrographs showing immunoreactivity for the α_{1A} subunit in the molecular layer of the cerebellum as detected by the pre-embedding immunoperoxidase method. (A and B) Peroxidase reaction end-product for α_{1A} could be observed in varicosities of parallel fibres (Pf), in parallel fibres (asterisks in A) and in climbing fibre (Cf) boutons. (B) Note that the reaction end-product was seen along the presynaptic membrane specialization of the CF varicosity. (C and D) Postsynaptically, immunostaining was found in Purkinje cell spines (s) establishing asymmetrical synapses with parallel fibre or climbing fibre varicosities. Scale bars, 0.2 μm.

peptide (2 μg/mL), no immunostaining was detected in sections of the rat cerebellum (data not shown).

Subcellular localization of the α_{1A} subunit

For electron microscopic investigation tissue blocks were taken from all the three layers of the cerebellum – molecular layer, PC layer and granule cell layer – but a detailed investigation of the localization of the α_{1A} subunit was carried out in the molecular layer where the functional properties of the P/Q-type calcium channels have been extensively studied. Similar specific immunolabelling was detected in rat and juvenile (P14) wild-type mice, but not in α_{1A}-deficient mice. Pre-embedding immunoperoxidase labelling revealed that the vast majority of PF varicosities were immunoreactive for the α_{1A} protein (Fig. 2A). Weak immunostaining was also seen in PFs (Fig. 2A) and in varicosities of CFs (Fig. 2B). The PF and CF varicosities were distinguished on the basis of their main morphological features: the PF varicosities contain round loosely aggregated synaptic vesicles and establish mostly single synapses with spines of distal dendrites of PCs, whereas CF varicosities are characterized by the dense packing of spherical vesicles and make several or more synapses with dendritic spines of proximal dendrites (Palay & Chan-Palay, 1974). Postsynaptically, virtually all PC spines were immunoreactive for the α_{1A} protein. Peroxidase reaction end-product for the channel subunit accumulated in dendritic spines postsynaptic to PF (Fig. 2C) and CF (Fig. 2D) varicosities. The dendritic shafts of PCs were also immunolabelled, but the density of the reaction product was consistently lower than that observed within the spines (data not shown). Using pre-embedding immunogold labelling, the highest density of immunoparticles for α_{1A} was found along the presynaptic membrane specialization of PF varicosities making asymmetrical synapses with dendritic spines of PC (Fig. 3A) and dendritic shafts (Fig. 3B) of presumed interneurons. A lower density of labelling was also detected on the extrasynaptic membrane of the varicosities (Fig. 3A and B) and in the preterminal portions of presumed PFs (Fig. 3C). The labelling in CF varicosities was also found along the presynaptic membrane specializations (Fig. 4). It was, however, consistently weaker in comparison with the immunoreactivity detected in PF varicosities. In postsynaptic elements, a high density of immunoparticles for α_{1A} was observed on the extrasynaptic plasma membrane of PC dendritic spines (Figs 3A and 5). Immunoparticles also appeared in perisynaptic position at the edge of asymmetrical synapses established by PF (Fig. 5A) and CF varicosities (data not shown) on dendritic spines of PCs. To test whether the α_{1A} subunit is localized over the postsynaptic specialization, we used the postembedding immunogold method, in which the antibodies have direct access to molecules present at the surface of the sections (Lujan *et al*., 1996). The antibody for the α_{1A} protein, however, failed to provide sufficiently strong immunolabelling under these experimental conditions. The labelling on dendritic shafts of PCs was sparse, and immunoparticles for α_{1A} localized to the extrasynaptic plasma membrane (Fig. 5B).

Immunoelectron microscopy further revealed that the immunostaining for α_{1A} in somata of PCs was due to the abundance of the protein in the endoplasmic reticulum. In the granule cell layer weak immunoreactivity for the subunit was found over the presynaptic membrane specialization of presumed mossy fibre axon terminals (data not shown). There was no immunostaining for the α_{1A} subunit in glial cells.

Quantification of α_{1A} immunoreactivity on pre- and postsynaptic membranes

The results obtained by pre-embedding methods demonstrated stronger immunoreactivity for the α_{1A} subunit of the P/Q-type calcium

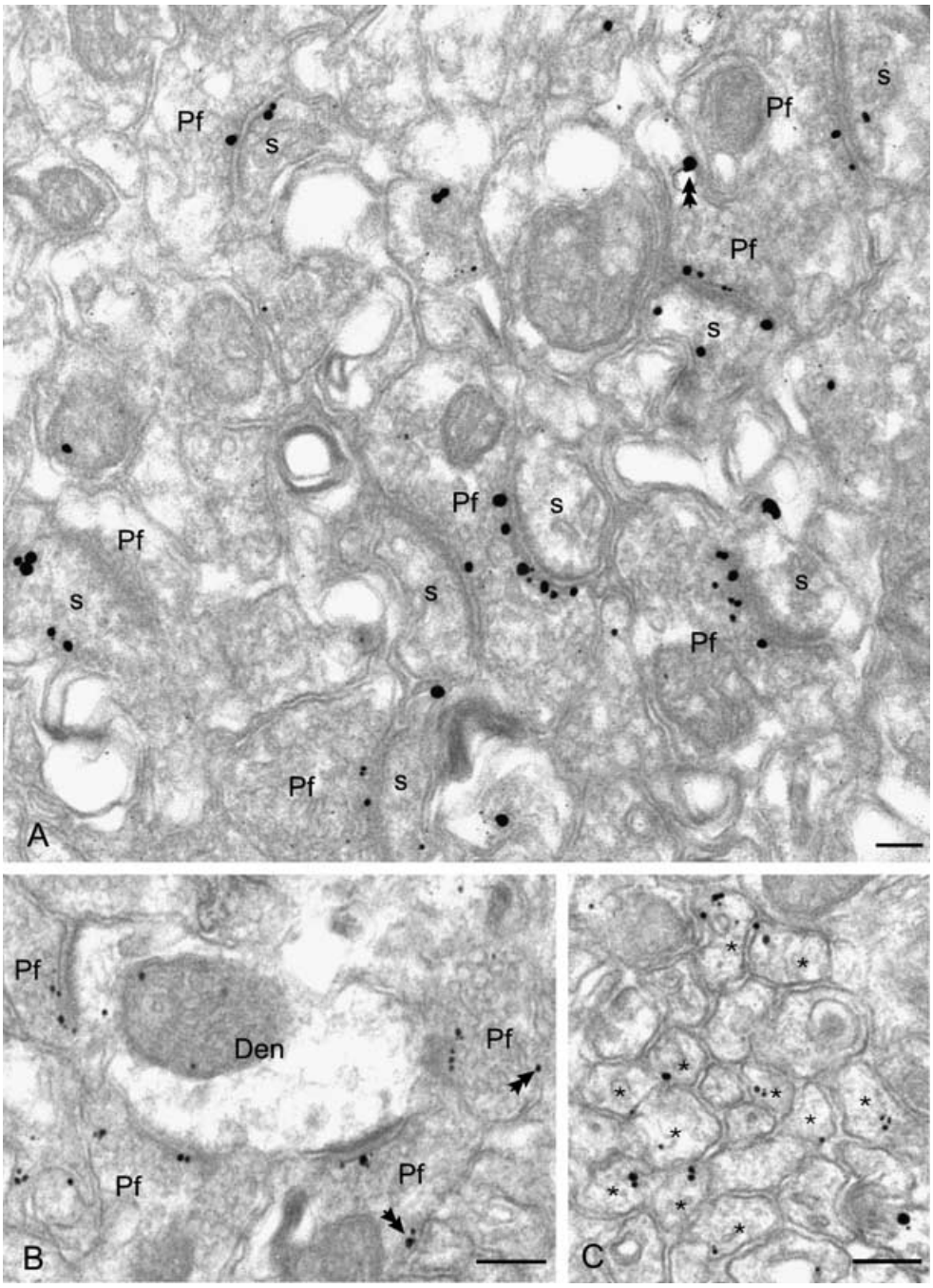

FIG. 3. Electron micrographs showing immunoreactivity for the α_{1A} subunit in parallel fibres as detected by the pre-embedding immunogold method. (A and B) Immunoparticles for α_{1A} were mainly localized to the presynaptic membrane specialization of parallel fibre varicosities (Pf) making asymmetrical synapses with either dendritic spines of Purkinje cells (s) or with dendritic shafts of presumed interneurons (Den). Occasionally, immunolabelling was detected on the extrasynaptic plasma membrane of parallel fibre varicosities (double arrows). (C) Immunoparticles for the α_{1A} subunit were also found in the preterminal portions of presumed parallel fibres (asterisks). Scale bars, 0.2 μm.

channel in varicosities than in axonal portions of PFs, and also over the presynaptic membrane specialization of PF varicosities than over that of CF varicosities. Furthermore, in postsynaptic elements the immunolabelling for the channel subunit was consistently stronger in dendritic spines than in dendritic shafts of PCs. In order to examine quantitatively the 3D distribution of the α_{1A} subunits relative to the PF–PC synapses and to compare the density of immunoparticles in PF and CF varicosities, PF varicosities (Fig. 6A), PFs (Fig. 6B), PC dendrites (Fig. 6C) and CF varicosities were reconstructed from serial ultrathin sections immunolabelled for α_{1A}. Overall, PFs, PC dendritic shafts and CF varicosities showed a low density of immunoparticles for α_{1A} [3.78 ± 1.39 particles/μm^2 in PFs ($n = 7$), 4.18 ± 2.01 particles/μm^2 in proximal ($n = 15$) and 6.65 ± 3.52 particles/μm^2 in distal ($n = 29$) PC dendrites, and 32 particles/μm^2 in CF varicosities ($n = 15$)], whereas PF varicosities (Fig. 6A) and PC dendritic spines (Fig. 6C) had much higher densities of immunoparticles, especially around the asymmetrical PF–PC synapses. A quantitative estimation of immunogold particles ($n = 287$) for α_{1A} in 60-nm-wide membrane segments of the reconstructed PF varicosities ($n = 10$) revealed a clear peak (217 particles/μm^2) of α_{1A} density within the presynaptic active

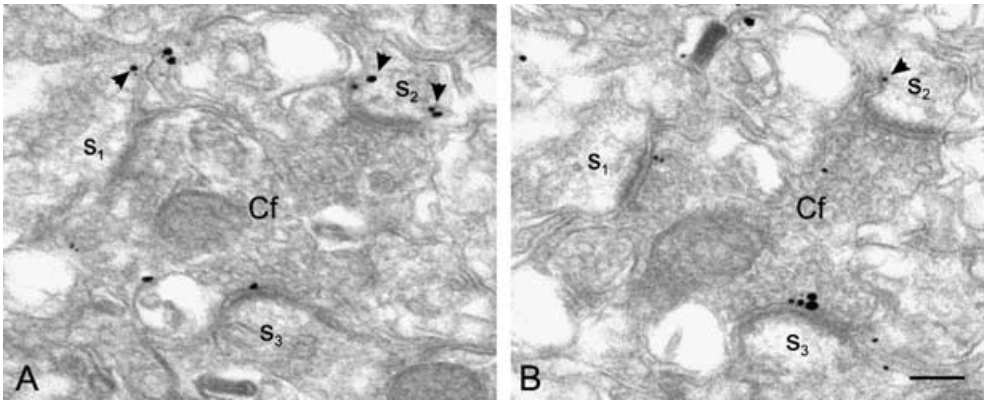

FIG. 4. Consecutive electron micrographs showing immunoreactivity for the α_{1A} subunit in a climbing fibre varicosity as assessed by the pre-embedding immunogold method. (A and B) Immunoparticles were localized to the presynaptic membrane specialization of the varicosity (Cf) establishing asymmetrical synaptic contacts with Purkinje cell dendritic spines (s_{1-3}). Note that spines were also immunolabelled (arrows). Scale bar, 0.2 μm.

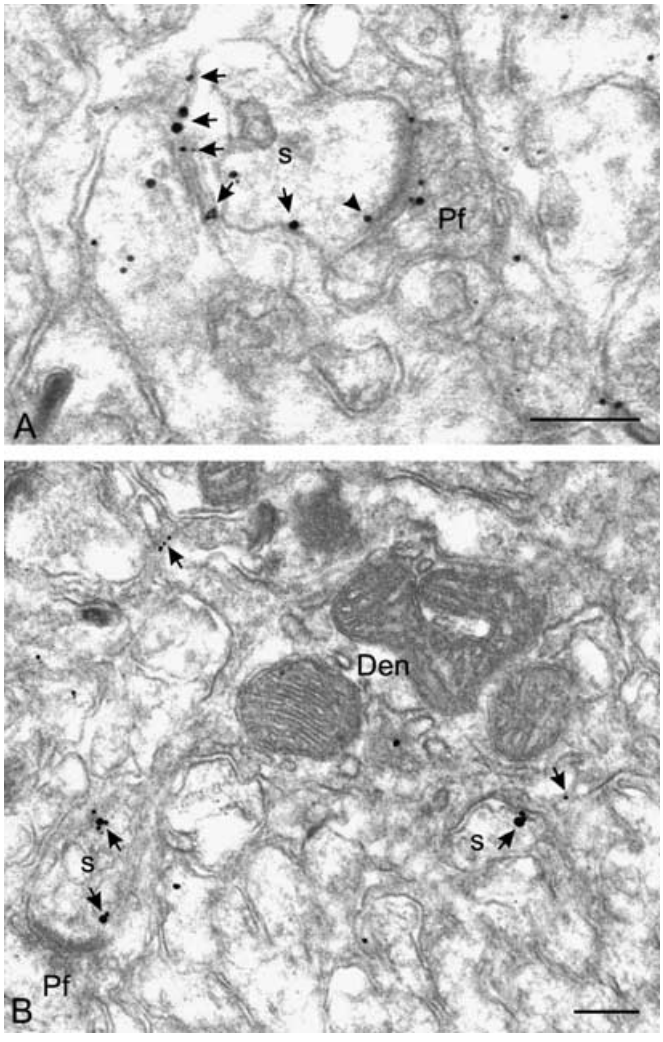

FIG. 5. Subcellular localization of the α_{1A} protein in dendritic spines and shafts of Purkinje cells as revealed by the pre-embedding immunogold method. (A and B) Immunoparticles were mainly present on the extrasynaptic plasma membrane (arrows) of Purkinje cell dendritic spine (s). Ocassionally, they also appeared at the edge of asymmetrical synapse (arrowhead in A) established by a parallel fibre varicosity (Pf) with the spine. Note that the presynaptic parallel fibre varicosity was also immunolabelled for α_{1A} over the presynaptic membrane specialization. (B) Immunoreactivity for α_{1A} was weak on the extrasynaptic membrane (arrows) of Purkinje cell dendritic shafts (Den). Scale bars, 0.2 μm.

zone with a steep decline of particle density outside the synapses (Fig. 6D). In dendritic spines of PCs ($n = 24$), immunoparticles ($n = 237$) for α_{1A} were concentrated (61–66 particles/μm^2) between 0 nm and 180 nm from the edge of asymmetrical synapses on the spines with a gradual decrease further away from synapses (Fig. 6E). These data indicate a close association of the P/Q-type calcium channels in both pre- and postsynaptic structures with neuronal elements serving glutamatergic transmission between PFs and PCs.

Localization of the α_{1A} subunit in GABAergic cells

It has recently been demonstrated that P/Q-type calcium channels have a role in mediating action potential-evoked inhibitory γ-aminobutyric acid (GABA) release on to mouse PCs (Stephens *et al.*, 2001). Furthermore, this channel type is considered to be responsible for a large fraction of the calcium rise in axons of GABAergic neurons during development (Forti *et al.*, 2000). To investigate the localization of the α_{1A} subunit in axons of GABAergic neurons, double immunolabelling was performed to co-visualize α_{1A} and GAD65, the GABA-synthesizing enzyme. These experiments revealed a weak immunogold labelling for α_{1A} in GAD-immunoreactive (GAD-IR) terminals: immunoparticles were found over the presynaptic membrane specialization of boutons and also localized to their extrasynaptic plasma membrane (Fig. 7A). No labelling was, however, detected in the preterminal portions of GAD-IR axons. To establish the ratio of the synaptic and extrasynaptic proteins, the location of immunogold particles for α_{1A} was investigated in serial ultrathin sections of axon terminals establishing symmetrical synaptic contact with dendritic shafts (Fig. 7Ba and Bb). These experiments revealed that approximately two-thirds of the immunoparticles (61%, $n = 20$) were found in the active zones of the terminals and one-third (39%, $n = 13$) were localized to the extrasynaptic plasma membrane.

Discussion

This study provides a detailed description of the precise subcellular localization of the α_{1A} subunit of the P/Q-type calcium channel in the rat cerebellum. We found a high density of the protein in the presynaptic active zone of PF varicosities and in the extrasynaptic membrane of PC dendritic spines. In contrast to the association of α_{1A} with the glutamatergic PF–PC synapses, immunoreactivity for this subunit was weak in CF varicosities, in dendritic shafts of PCs and in axon terminals of GABAergic neurons. The association of the P/Q-type channel with glutamatergic synapses at both pre- and

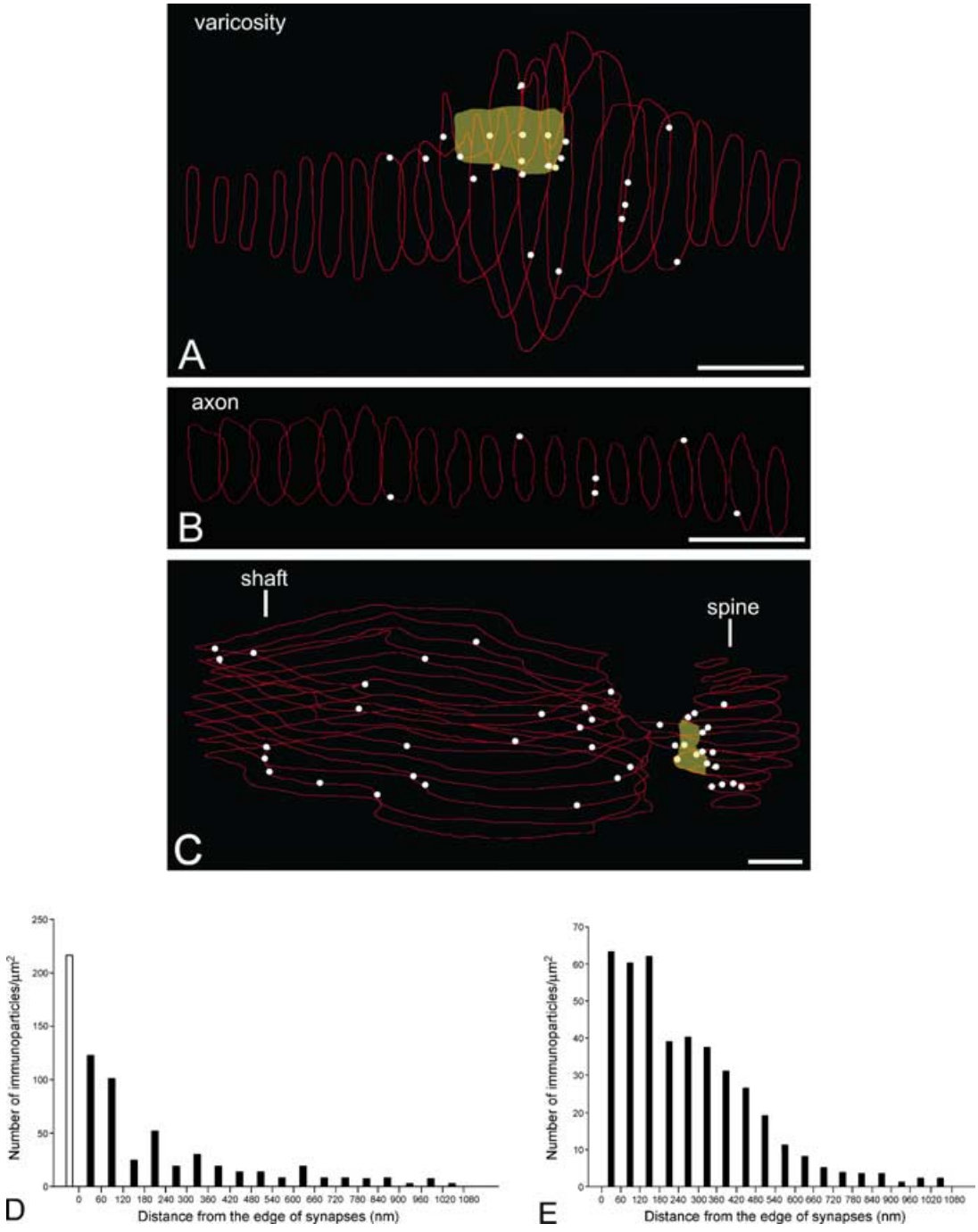

FIG. 6. Distribution of the α_{1A} subunit in parallel fibres and Purkinje cells as shown by three-dimensional (3D) reconstruction and determined by quantification of immunogold density. (A–C) Three-dimensional reconstruction of a parallel fibre varicosity (A), preterminal portion of a parallel fibre (B), and a Purkinje cell dendritic shaft with a spine (C) was carried out from serial ultrathin sections ($n = 22$ in A, $n = 19$ in B, $n = 14$ in C), obtained from pre-embedding material, showing the localization of immunogold particles for α_{1A} (white dots) in relation to the asymmetrical synaptic junctions (yellow area) and the distribution of the α_{1A} subunit along the axonal membrane (B). (A) In the parallel fibre varicosity, immunoparticles for α_{1A} were concentrated within the asymmetrical synaptic junction. (B) In the parallel fibre, immunogold particles for α_{1A} were distributed sparsely along the plasma membrane. (C) In the Purkinje cell dendrite, most of the immunogold particles for the α_{1A} were located in the spine particularly around the asymmetrical synapses (yellow area) with parallel fibre inputs. (D) Graph showing the distribution of immunoparticles ($n = 278$) for the α_{1A} in parallel fibre varicosities ($n = 10$) relative to asymmetrical, glutamatergic synapses established with Purkinje cell dendritic spines. Distances between immunoparticles and the closest edge of synapses were measured along the 3D reconstructed images. Immunoparticles collected from varicosities were allocated to 60-nm-wide bins along the surface of the reconstructed images starting at the edge of asymmetrical synapses. The number of particles in each bin was divided by the sampled area to calculate the density of immunoparticles. The result demonstrates a clear peak over the presynaptic membrane specialization (open column). (E) Graph showing the distribution of immunoparticles ($n = 237$) for the α_{1A} subunit in Purkinje cell dendritic spines ($n = 24$) relative to asymmetrical synapses established with parallel fibres. The measurement and the calculation of the density of immunoparticles followed the method described above for parallel fibres. This measurement demonstrates a peak of α_{1A} labelling density between 0 nm and 180 nm from the edge of asymmetrical synapses on spines. Scale bars, 0.3 µm.

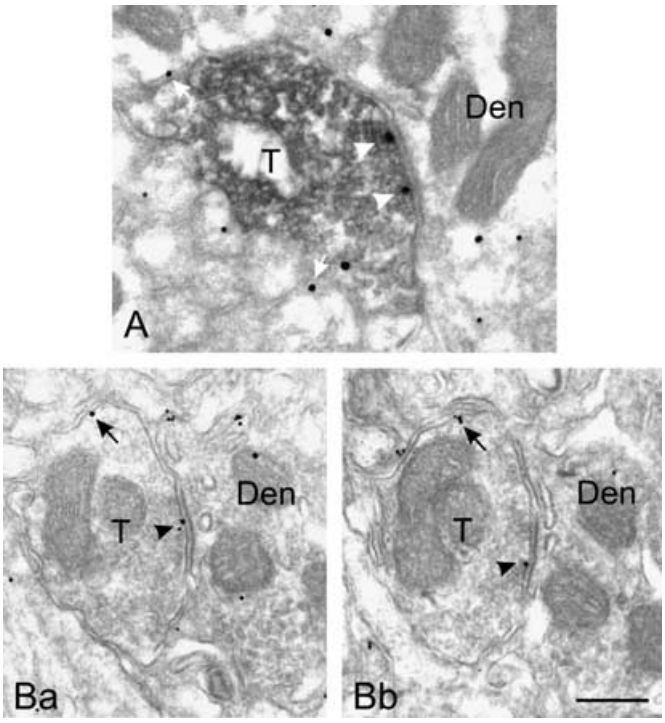

FIG. 7. Electron micrographs showing immunoreactivity for the α_{1A} subunit in axon terminals of GABAergic cells as revealed by the pre-embedding immunogold method. (A) Immunogold particles for α_{1A} were found on the presynaptic membrane specialization (arrowheads) and also at the extrasynaptic plasma membrane (arrows) of a glutamic acid decarboxylase-immunoreactive (peroxidase reaction end-product) axon terminal (T). (Ba and Bb) Consecutive electron micrographs showing immunoreactivity for α_{1A} in an axon terminal (T) making symmetrical synapse with a dendritic shaft (Den). Approximately two-thirds of the immunoparticles in such terminals with symmetrical synapses were located on the active zone and the rest in the extrasynaptic plasma membrane of these terminals. Scale bar, 0.2 μm.

postsynaptic sites suggests their involvement in diversified regulation of the excitatory neurotransmission between PFs and PCs.

Cellular distribution of the α_{1A} subunit

The immunohistochemical distribution pattern of the α_{1A} subunit in the cerebellum, detected at the light microscopic level, appears to be consistent with the distribution of binding sites for ω-Aga-IVA, a specific potent blocker of the P/Q-type channel, in the cerebellar cortex (Nakanishi *et al*., 1995). The strong immunolabelling, observed in the molecular layer, is mainly ascribable to the abundance of α_{1A} in PF varicosities and in PC dendritic spines. In addition, weak immunostaining was also detected in CF varicosities, in terminals of GABAergic cells and in dendritic shafts of PCs. These findings are in agreement with *in situ* hybridization studies reporting a high expression of α_{1A} mRNA in granule cells and PCs, and a much lower expression level of the protein in neurons of the inferior olive and in cells of the cerebellar molecular layer (Stea *et al*., 1994; Tanaka *et al*., 1995; Ludwig *et al*., 1997; Craig *et al*., 1998).

Presynaptic α_{1A} subunits are on excitatory and inhibitory terminals

The PFs evoke a small calcium transient in PCs, whereas CFs exert a powerful influence on the firing of PCs (Konnerth *et al*., 1992). The PF–PC synapses are characterized by a low release probability, whereas CF–PC synapses have a high release probability (Silver *et al*., 1998). The neurotransmitter release is steeply dependent upon calcium influx (Mintz *et al*., 1995) through calcium channels (Regehr & Mintz, 1994; Mintz *et al*., 1995; Randall & Tsien, 1995). In this study the α_{1A} subunits were found on the presynaptic membrane specialization of both PF and CF varicosities. This finding agrees well with the effect of ω-Aga-IVA, which decreased the presynaptic calcium entry by 50% in PFs (Mintz *et al*., 1995) and reduced synaptic strength by 77% at CF–PC synapses (Regehr & Mintz, 1994). Direct binding of α_{1A} with a synaptic vesicle protein, synaptotagmin I (Charvin *et al*., 1997) and with synaptic plasma membrane SNARE proteins (Zhong *et al*., 1999) further supports the role of the P/Q-type channels in transmitter release. Evidence suggests that multiple types of calcium channels contribute to neurotransmitter release at a single release site (Borst & Sakmann, 1996; Wu & Saggau, 1997). Among these channels, P/Q-type was demonstrated to be more efficient in triggering neurotransmitter release than other calcium channels at hippocampal synapses (Luebke *et al*., 1993; Takahashi & Momiyama, 1993; Castillo *et al*., 1994; Wheeler *et al*., 1994) and cerebellar synapses (Takahashi & Momiyama, 1993; Regehr & Mintz, 1994; Mintz *et al*., 1995). This may be partly due to the closer association of α_{1A} to the site of vesicle fusion, as found in the present study, than other subunits (Wu *et al*., 1999).

Despite a major role of P/Q-type channels in neurotransmitter release in both PFs and CFs (Doroshenko *et al*., 1997), a lower density of immunoreactivity for α_{1A} was found in CF varicosities (32 particles/μm^2) than in PF varicosities (217 particles/μm^2) in the present study. However, mRNAs for distinct sets of α_1 subunits were found in cerebellar granule cells and in neurons of the inferior olive (Tanaka *et al*., 1995; Ludwig *et al*., 1997) and the extent of contribution of α_{1A} to the regulation of glutamate release from PF and CF varicosities may depend on the relative abundance of α_{1A} in the whole population of α_1 subunits involved in the release. In addition, we should consider the existence of electrophysiologically distinct P/Q-type channels in varicosities based on a distinct subunit composition, i.e. different β subunits (Castellano & Perez-Reyes, 1992) may be associated with the pore-forming α_{1A} subunit. Previous studies demonstrated that different β subunits can differentially modulate the kinetic properties of the calcium current generated by the α_{1A} subunit (Stea *et al*., 1994; De Waard & Campbell, 1995). Although decisive immunohistochemical study is not available on the subunit composition of functional P/Q-type channels, *in situ* hybridization studies revealed different expression patterns of different β subunit splice variants in the cerebellar granule cells and in the inferior olive (Tanaka *et al*., 1995; Ludwig *et al*., 1997). This raises the possibility that P/Q-type channels located to PF varicosities are different in their subunit composition and kinetics from those localized to CF varicosities.

Some studies proposed that inhibitory interneurons of the molecular layer do not posses the α_{1A} subunit (Tanaka *et al*., 1995; Doroshenko *et al*., 1997). By contrast, others revealed the expression of α_{1A} in cells of the molecular layer (Ludwig *et al*., 1997; Craig *et al*., 1998), reporting that P/Q-type channels have a role in mediating action potential-evoked inhibitory GABA release on to mouse PCs (Stephens *et al*., 2001), and showing hot spots of P/Q-type channels along axons of immature basket and stellate cells, which may be responsible for a large fraction of the axonal calcium rise (Forti *et al*., 2000). Our immunocytochemical data, showing the location of α_{1A} in the active zone and at the extrasynaptic plasma membrane of GABAergic terminals, are in line with the results of these latter studies. The labelling for this subunit, however, was weak and restricted to axon terminals, seemingly different from the distribution pattern proposed in calcium imaging study (Forti *et al*., 2000). This discrepancy may reflect a decrease in P/Q-type channel density during axonal maturation as it has been observed for the α_{1A} transcripts in cerebellar

cultures (Falk *et al*., 1999) and/or subcellular redistribution of the channels during neuronal development.

Dendritic localization of the α_{1A} subunit in Purkinje cells

Virtually all PCs were found to be immunoreactive for α_{1A}. This favours the finding of Mintz *et al*. (1992a), who showed that bath application of ω-Aga-IVA almost completely abolished the high threshold currents in all PCs. The dendritic localization of the α_{1A} protein is in agreement with observations of electrophysiological studies demonstrating that the depolarization-induced generation of dendritic calcium transients, evoked by the activation of PFs and CFs, is partially due to the calcium influx through voltage-activated calcium channels (Tank *et al*., 1988; Konnerth *et al*., 1992; Denk *et al*., 1995; Eilers *et al*., 1995, 1996; Wang *et al*., 2000), probably via the most abundant P-type channels (Mintz *et al*., 1992a). In the present study, the majority of the α_{1A} subunits were localized to spines with the highest density at sites of the extrasynaptic membrane between 0 nm and 180 nm away from the synaptic membrane specialization of putative glutamatergic synapses. Using similar quantitative immunocytochemical techniques, two subtypes of G-protein-coupled metabotropic receptors, $GABA_{B1}$ and mGluR1a, have recently been shown at extrasynaptic sites of PC spines, peaking at 180–240 nm ($GABA_{B1}$) and concentrated within 60 nm (mGluR1a) from the edge of the PF–PC synapses (Luján *et al*., 1997; Kulik *et al*., 2002). The location of α_{1A} near membrane areas to which $GABA_{B1}$ and mGluR1a are localized is in accordance with findings proposing a role of metabotropic receptors in the regulation of P/Q-type channels in controlling dendritic calcium transients in PCs. Thus, whole-cell patch recording showed that P-type channels are inhibited by $GABA_B$ receptors through a G-protein-mediated mechanism (Mintz & Bean, 1993), suggesting their involvement in the hyperpolarization of PCs. Regarding the close apposition of α_{1A} and mGluR1a, it has recently been demonstrated that the two proteins form a heteromeric complex through direct protein–protein interaction between their intracellular domains (Kitano *et al*., 2003). Expression and pre-activation of mGluR1 alone inhibits the α_{1A} subunit-mediated increase of intracellular calcium concentration in the absence of mGluR1 activation, whereas simultaneous stimulation of the glutamate receptor and the ion channel induces a large increase in calcium concentration (Kitano *et al*., 2003). Such synergistic effects of α_{1A} and mGluR1 activation on intracellular calcium concentration would be advantageous for the induction of LTD in PF–PC synapses. Furthermore, it was recently reported that, in addition to mGluR1-mediated inositol-1,4,5-triphosphate (IP_3) production, the depolarization, mediated by AMPA receptor activation, and the resultant calcium influx via calcium channels – preferentially through P-type channels – induces IP_3 production in PCs (Okubo *et al*., 2001). The activation of IP_3 receptors (IP_3Rs) results in calcium release from internal stores of PC spines generating a supralinear calcium signal (Okubo *et al*., 2001). Thus, P-type channels in spines have a strategic position to activate IP_3Rs in a synergistic manner with mGluR1.

In conclusion, the present study demonstrates the apparent association of the α_{1A} subunit of the P/Q-type calcium channel with the glutamatergic synapses, suggesting that these channels play a role in the regulation of excitatory neurotransmission and contribute to the generation of postsynaptic calcium transport. Consequently, P/Q-type channels are likely to be involved in the induction of cerebellar LTD that underlies the cerebellar motor learning.

Acknowledgements

We are grateful to Drs Akiko Momiyama and Imre Vida for their helpful suggestions on the manuscript. We thank Aniko Schneider, Sigrun Nestel and Renate Wirtz for their support with electron microscopy. This work was supported by the DFG: SFB 505. A.K. was supported by the Alexander von Humboldt Foundation.

Abbreviations

ABC, avidin–biotin complex; AMPA, α-amino-3-hydroxy-5-methyl-4-isoxazolepropionic-acid; BSA, bovine serum albumin; CF, climbing fibre; 3D, three-dimensional; DAB, 3-3′-diaminobenzidine tetrahydrochloride; EPSP, excitatory postsynaptic potential; GABA, γ-aminobutyric acid; $GABA_{B1}$, γ-aminobutyric acid receptor subunit 1; GAD, glutamic acid decarboxylase; GAD-IR, GAD-immunoreactive; HRP, horseradish peroxidase; HVA, high voltage-activated; IP_3, inositol-1,4,5-triphosphate; IP_3R, inositol-1,4,5-triphosphate receptor; LTD, long-term depression; mGluR1, metabotropic glutamate receptor subtype 1; mRNA, messenger ribonucleic acid; NGS, normal goat serum; PB, phosphate buffer; PBS, phosphate-buffered saline; PC, Purkinje cell; PF, parallel fibre; PVDF, polyvinylidene diflouride; SDS-PAGE, sodium dodecyl sulphate-polyacrylamide gel electrophoresis; SNARE, soluble N-ethylmaleimide-sensitive factor attachment protein receptor; TB, tris buffer; TBS, tris-buffered saline; TRI, three-dimensional reconstruction imaging.

References

Borst, J.G. & Sakmann, B. (1996) Calcium influx and transmitter release in a fast CNS synapse. *Nature*, **383**, 431–434.

Castellano, A. & Perez-Reyes, E. (1992) Molecular diversity of Ca^{2+} channel β subunits. *Biochem. Soc. Trans.*, **22**, 483–487.

Castillo, P.E., Weisskopf, M.G. & Nicoll, R.A. (1994) The role of Ca^{2+} channels in hippocampal mossy fiber synaptic transmission and long-term potentiation. *Neuron*, **12**, 261–269.

Catterall, W.A. (1998) Structure and function of neuronal Ca^{2+} channels and their role in neurotransmitter release. *Cell Calcium*, **24**, 307–323.

Catterall, W.A. (2000) Structure and regulation of voltage-gated Ca^{2+} channels. *Annu. Rev. Cell Dev. Biol.*, **16**, 521–555.

Charvin, N., Leveque, C., Walker, D., Berton, F., Raymond, C., Kataoka, M., Shoji-Kasai, Y., Takahashi, M., De Waard, M. & Seagar, M.J. (1997) Direct interaction of the calcium sensor protein synaptotagmin I with a cytoplasmic domain of the α_{1A} subunit of the P/Q-type calcium channel. *EMBO J.*, **16**, 4591–4596.

Craig, P.J., McAinsh, A.D., McCormack, A.L., Smith, W., Beattie, R.E., Priestley, J.V., Lai Yee Yip, J., Averill, S., Longbottom, E.R. & Volsen, S.G. (1998) Distribution of the voltage-dependent calcium channel α_{1A} subunit throughout the mature rat brain and its relationship to neurotransmitter pathways. *J. Comp. Neurol.*, **397**, 251–267.

De Schutter, E. & Bower, J.M. (1994) Simulated responses of cerebellar Purkinje cells are independent of the dendritic location of granule cell synaptic inputs. *Proc. Natl Acad. Sci. USA*, **91**, 4736–4740.

De Waard, M. & Campbell, K.P. (1995) Subunit regulation of the neuronal α_{1A} Ca^{2+} channel expressed in *Xenopus oocytes*. *J. Physiol. (Lond.)*, **485**, 619–634.

Denk, W., Sugimori, M. & Llinas, R. (1995) Two types of calcium response limited to single spines in cerebellar Purkinje cells. *Proc. Natl Acad. Sci. USA*, **92**, 8279–8282.

Doroshenko, P.A., Woppmann, A., Miljanich, G. & Augustine, G.J. (1997) Pharmacologically distinct presynaptic calcium channels in cerebellar excitatory and inhibitory synapses. *Neuropharmacology*, **36**, 865–872.

Dunlap, K., Luebke, J.I. & Turner, T.J. (1995) Exocytotic Ca^{2+} channels in mammalian central neurons. *Trends Neurosci.*, **18**, 89–98.

Eilers, J., Augustine, G.J. & Konnerth, A. (1995) Subthreshold synaptic Ca^{2+} signalling in fine dendrites and spines of cerebellar Purkinje neurons. *Nature*, **373**, 155–158.

Eilers, J., Plant, T. & Konnerth, A. (1996) Localized calcium signalling and neuronal integration in cerebellar Purkinje neurones. *Cell Calcium*, **20**, 215–226.

Falk, T., Muller, L.Y. & Yool, A.J. (1999) Differential expression of three classes of voltage-gated Ca^{2+} channels during maturation of the rat cerebellum in vitro. *Dev. Brain Res.*, **115**, 161–170.

Forti, L., Pouzat, C. & Llano, I. (2000) Action potential-evoked Ca^{2+} signals and calcium channels in axons of developing rat cerebellar interneurons. *J. Physiol. (Lond.)*, **527**, 33–48.

Hartell, N.A. (1996) Strong activation of parallel fibers produces localized calcium transients and a form of LTD that spreads to distant synapses. *Neuron*, **16**, 601–610.

Jones, S.W. (1998) Overview of voltage-dependent calcium channels. *J. Bioenerg. Biomemb.*, **30**, 299–312.

Jun, K., Piedras-Renteria, E.S., Smith, S.M., Wheeler, D.B., Lee, S.B., Lee, T.G., Chin, H., Adams, M.E., Scheller, R.H., Tsien, R.W. & Shin, H.-S. (1999) Ablation of P/Q-type Ca^{2+} channel currents, altered synaptic transmission, and progressive ataxia in mice lacking the α_{1A}-subunit. *Proc. Natl Acad. Sci. USA*, **96**, 15245–15250.

Kitano, J., Nishida, M., Itsukaichi, Y., Minami, I., Ogawa, M., Hirano, T., Mori, Y. & Nakanishi, S. (2003) Direct interaction and functional coupling between metabotropic glutamate receptor subtype 1 and voltage-sensitive $Ca_v2.1$ Ca^{2+} channel. *J. Biol. Chem.*, **278**, 25101–25108.

Konnerth, A., Dreesen, J. & Augustine, G.J. (1992) Brief dendritic calcium signals initiate long-lasting synaptic depression in cerebellar Purkinje cell. *Proc. Natl Acad. Sci. USA*, **89**, 7051–7055.

Kulik, A., Nakadate, K., Nyiri, G., Notomi, T., Malitschek, B., Bettler, B. & Shigemoto, R. (2002) Distinct localization of $GABA_B$ receptors relative to synaptic sites in the rat cerebellum and ventrobasal thalamus. *Eur. J. Neurosci.*, **15**, 291–307.

Ludwig, A., Flockerzi, V. & Hofmann, F. (1997) Regional expression and cellular localization of the α_1 and β subunit of high voltage-activated calcium channels in rat brain. *J. Neurosci.*, **17**, 1339–1349.

Luebke, J.I., Dunlap, K. & Turner, T.J. (1993) Multiple calcium channel types control glutamatergic synaptic transmission in the hippocampus. *Neuron*, **11**, 895–902.

Lujan, R., Nusser, Z., Roberts, J.D.B., Shigemoto, R. & Somogyi, P. (1996) Presynaptic location of metabotropic glutamate receptors mGluR1 and mGluR5 on dendrites and dendritic spines in the rat hippocampus. *Eur. J. Neurosci.*, **8**, 1488–1500.

Luján, R., Roberts, J.D.B., Shigemoto, R., Ohishi, H. & Somogyi, P. (1997) Differential plasma membrane distribution of metabotropic glutamate receptors mGluR1a, mGluR2 and mGluR5, relative to neurotransmitter release sites. *J. Chem. Neuroanat.*, **13**, 219–241.

Matsushita, K., Wakamori, M., Rhyu, I.J., Arii, T., Oda, S.-I., Mori, Y. & Imoto, K. (2002) Bidirectional alterations in cerebellar synaptic transmission of *tottering* and *rolling* Ca^{2+} channel mutant mice. *J. Neurosci.*, **22**, 4388–4398.

Miller, R.J. (1987) Multiple calcium channels and neuronal function. *Science*, **235**, 46–52.

Mintz, I.M., Adams, M.E. & Bean, B.P. (1992a) P-type calcium channels in rat central and peripheral neurons. *Neuron*, **9**, 85–95.

Mintz, I.M. & Bean, B.P. (1993) $GABA_B$ receptor inhibition of P-type Ca^{2+} channels in central neurons. *Neuron*, **10**, 889–898.

Mintz, I.M., Sabatini, B.L. & Regehr, W.G. (1995) Calcium control of transmitter release at a cerebellar synapse. *Neuron*, **15**, 675–688.

Mintz, I.M., Venema, V.J., Swiderek, K.M., Lee, T., Bean, B.P. & Adams, M.E. (1992b) P-type calcium channels blocked by the spider toxin ω-Aga-IVA. *Nature*, **355**, 827–829.

Mori, Y., Friedrich, T., Kim, M.-S., Mikami, A., Nakai, J., Ruth, P., Bosse, E., Hofmann, F., Flockerzi, V., Furuichi, T., Mikoshiba, K., Imoto, K., Tanabe, T. & Numa, S. (1991) Primary structure and functional expression from complementary DNA of a brain calcium channel. *Nature*, **350**, 398–402.

Nakanishi, S., Fujii, A., Kimura, T., Sakakibara, S. & Mikoshiba, K. (1995) Spatial distribution of ω-Agatoxin IVA binding sites in mouse brain slices. *J. Neurosci. Res.*, **41**, 532–539.

Okubo, Y., Kakizawa, S., Hirose, K. & Iiono, M. (2001) Visualization of IP(3) dynamics reveals a novel AMPA receptor-triggered IP(3) production pathway mediated by voltage-dependent Ca(2+) influx in Purkinje cells. *Neuron*, **32**, 113–122.

Palay, S.L. & Chan-Palay, V. (1974) *Cerebellar Cortex. Cytology and Organization*. Springer-Verlag, Berlin.

Randall, A. & Tsien, R.W. (1995) Pharmacological dissection of multiple types of Ca^{2+} channel currents in rat cerebellar granule neurons. *J. Neurosci.*, **15**, 2995–3012.

Regehr, W.G. & Mintz, I.M. (1994) Participation of multiple calcium channel types in transmission at single climbing fiber to Purkinje cell synapses. *Neuron*, **12**, 605–613.

Silver, R.A., Momiyama, A. & Cull-Candy, S.G. (1998) Locus of frequency-dependent depression identified with multiple-probability fluctuation analysis at rat climbing fibre-Purkinje cell synapses. *J. Physiol. (Lond.)*, **510**, 881–902.

Starr, T.V.B., Prystay, W. & Snutch, T.P. (1991) Primary structure of a calcium channel that is highly expressed in the rat cerebellum. *Proc. Natl Acad. Sci. USA*, **88**, 5621–5625.

Stea, A., Tomlinson, W.J., Soong, T.W., Bourinet, E., Dubel, S.J., Vincent, S.R. & Snutch, T.P. (1994) Localization and functional properties of a rat brain α_{1A} calcium channel reflect similarities to neuronal Q- and P-type channels. *Proc. Natl Acad. Sci. USA*, **91**, 10576–10580.

Stephens, G.J., Morris, N.P., Fyffe, R.E.W. & Robertson, B. (2001) The $Ca_v2.1$/α_{1A} (P/Q-type) voltage-dependent calcium channel mediates inhibitory neurotransmission onto mouse cerebellar Purkinje cell. *Eur. J. Neurosci.*, **13**, 1902–1912.

Takahashi, T. & Momiyama, A. (1993) Different types of calcium channels mediate central synaptic transmission. *Nature*, **366**, 156–158.

Tanaka, O., Sakagami, H. & Kondo, H. (1995) Localization of mRNAs of voltage-dependent Ca^{2+} channels: four subtypes of α_1- and β-subunits in developing and mature rat brain. *Mol. Brain Res.*, **30**, 1–16.

Tank, D.W., Sugimori, M., Connor, J.A. & Llinas, R.R. (1988) Spatially resolved calcium dynamics of mammalian Purkinje cells in cerebellar slice. *Science*, **242**, 773–777.

Usowicz, M.M., Sugimori, M., Cherksey, B. & Llinas, R. (1992) P-type calcium channels in the somata and dendrites of adult cerebellar Purkinje cells. *Neuron*, **9**, 1185–1199.

Wang, S.S.-H., Denk, W. & Häusser, M. (2000) Coincidence detection in single dendritic spines mediated by calcium release. *Nat. Neurosci.*, **12**, 1266–1273.

Westenbroek, R.E., Sakurai, T., Elliott, E.M., Hell, J.W., Starr, T.V.B., Snutch, T.P. & Catterall, W.A. (1995) Immunochemical identification and subcellular distribution of the α_{1A} subunits of brain calcium channels. *J. Neurosci.*, **15**, 6403–6418.

Wheeler, D.B., Randall, A. & Tsien, R.W. (1994) Roles of N-type and Q-type Ca^{2+} channels in supporting hippocampal synaptic transmission. *Science*, **264**, 107–111.

Wu, L.-G. & Saggau, P. (1997) Presynaptic inhibition of elicited neurotransmitter release. *Trends Neurosci.*, **20**, 204–212.

Wu, L.-G., Westenbroek, R.E., Borst, J.G.G., Catterall, W.A. & Sakmann, B. (1999) Calcium channel types with distinct presynaptic localization couple differentially to transmitter release in single calyx-type synapses. *J. Neurosci.*, **19**, 726–736.

Zhong, H., Yokoyama, C.T., Scheuer, T. & Catterall, W.A. (1999) Reciprocal regulation of P/Q-type Ca^{2+} channels by SNAP-25, syntaxin and synaptotagmin. *Nat. Neurosci.*, **2**, 939–941.